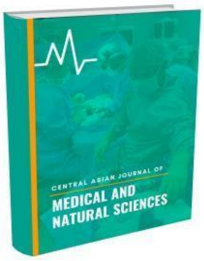

CENTRAL ASIAN JOURNAL OF
MEDICAL AND NATURAL SCIENCES
https://cajmns.centralasianstudies.org/index.php/CAJMNS
Volume: 07 Issue: 03 | July 2026 ISSN: 2660-4159

.

Articley

Integration of Geophysical and Hydrochemical Methods of Slabiat Depression, Southern Iraq

Aqeel Rahman Hasan[*1]

1. Iraqi Ministry of Education, AL-Muthanna Education Directorate
* Correspondence: akeelrahmen@Gmail.com

Abstract: The research location is situated in southern Iraq's Slabiat Depression. The WQI (Water Quality Index) and the 2D resistivity approach are the two techniques used to assess the water quality. Nineteen water samples are taken from wells in different parts of the Slabiat depression. pH, total dissolved solids (TDS), electrical conductivity (EC), total hardness (TH), calcium (Ca^{2+}), sodium (Na^{+}), magnesium (Mg^{2+}), chloride (Cl^{-}), sulfate (SO_4^{2-}), bicarbonate (HCO_3^{-}), and nitrate (NO_3^{-} ,are among the physiochemical characteristics that are examined. The results indicate that while the majority of the samples surpass Iraqi standards, the pH and nitrate (NO_3^{-}) concentrations are within normal limits. According to the WQI, which ranges from 73.12 to 117.7, water quality is categorized as poor to unfit for human consumption. To identify the groundwater aquifers, three two-dimensional resistivity profiles are used. The RES2DINV program processes and interprets 2D resistivity data using a reliable inversion technique. The study region is divided into three primary resistivity zones. Quaternary deposits were represented by the first resistivity zone, which was located at shallow depth and ranged between 2.00 and 10.1 ohm.m. The second resistivity zone, which is found in the center of the Dammam Formation, indicates the bearing-groundwater zone and ranges from 22.8 to 51.3 ohm.m. The impermeability zone of the lower Dammam Formation is represented by the third resistivity zone, which ranged from 115 to 584 ohm.m.

Keywords: Geophysical, Hydrochemical, Slabiat Depression, Iraq.

Citation: Hasan A. R. Integration of Geophysical and Hydrochemical Methods of Slabiat Depression, Southern Iraq. Central Asian Journal of Medical and Natural Science 2026, 7(3), 682-695.

Received: 24th Mar 2026
Revised: 14th Apr 2026
Accepted: 07th May 2026
Published: 23rd Jun 2026

Copyright: © 2026 by the authors. Submitted for open access publication under the terms and conditions of the Creative Commons Attribution (CC BY) license (https://creativecommons.org/licenses/by/4.0/)

1. Introduction

Water is a vital and irreplaceable natural resource that sustains life on Earth, and maintaining its quality is fundamental to environmental sustainability and human well-being. Ensuring the availability of high-quality water resources for future generations requires continuous protection of both water quantity and quality . Climatic conditions significantly influence water quality in any region, making water balance calculations essential for understanding and managing hydrological processes and environmental changes [1]. Effective management and planning of water resources are therefore necessary to mitigate the impacts of climatic variability, particularly fluctuations in rainfall and temperature patterns . Since water quality directly affects human health and socioeconomic development, appropriate measures must be adopted to ensure its safe and sustainable use [2].

In the Slabiat Depression, increasing population growth, urban expansion, and industrial activities have intensified the demand for groundwater resources, leading to overexploitation and potential contamination. Consequently, continuous monitoring and assessment of groundwater quality are essential for the sustainable management and protection of these resources. Various techniques have been employed to evaluate groundwater quality, including physical, chemical, and biological methods. Among these, the Water Quality Index (WQI) is one of the most widely applied approaches, as it combines multiple water quality parameters into a single numerical value that reflects the overall suitability of groundwater for use [3].

In addition to hydrochemical assessments, geophysical methods have proven effective in detecting groundwater contamination. The electrical resistivity method is a widely used, non-invasive geophysical technique for investigating subsurface conditions and identifying potential groundwater and soil contamination without the need for drilling boreholes or collecting extensive soil and water samples . This method offers several advantages, including rapid data acquisition, cost-effectiveness, and improved imaging of subsurface structures. Contaminants such as sewage water, which contain elevated concentrations of dissolved salts and organic matter, typically exhibit lower electrical resistivity than uncontaminated soils and groundwater. Therefore, zones characterized by low resistivity anomalies can indicate the presence and spatial extent of sewage-related contamination [4].

Accordingly, this study aims to assess groundwater quality and identify potential contamination zones in the Slabiat Depression through the integrated application of the Water Quality Index (WQI) and the electrical resistivity method.

Location of Study Area:

Slabiat Depression is located in southern Iraq, between longitudes 45º 34' and 45º 52' and latitudes 30º 50' and 30º 59'. It is administratively divided between the Muthanna and Dhi Qar governorates, situated to the right of the Euphrates River and about 40 km west of the city of Al-Khader Fig. **(1).**

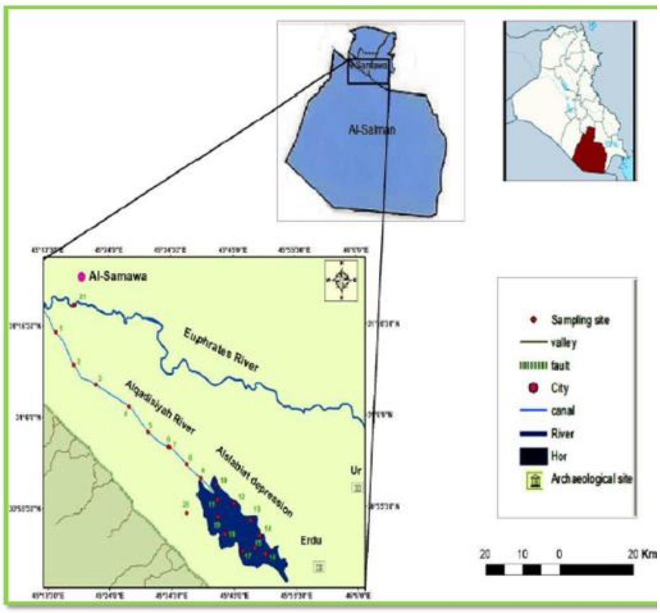

Figure 1. Location og study area.

The study area is located along the transitional zone between the desert plateau and the alluvial plain of southern Iraq. Historically, the Euphrates River flowed through this depression, passing between the ancient city of Eridu on its left bank and the archaeological site of Tell Lahm on its right bank before continuing across the alluvial plain toward the Hammar Marshes. The formation of the depression is attributed to tectonic activities that extended from the Tertiary period through the Holocene epoch.

The Slabiat Depression functions as a natural reservoir for excess Euphrates floodwaters and surface runoff originating from the surrounding valleys. To enhance water conveyance in the region, the Qadisiyah artificial canal was constructed and opened at the end of 1991, with the project completed within approximately six months. The canal extends for about 88 km, linking the Atshan River to the Slabiat Depression, and represents the principal water source in the area. It supplies irrigation water to approximately 8,500 dunums of agricultural land and supports livestock activities, particularly sheep and camel breeding. Along the stretch extending from Al-Masfaa Bridge to the Slabiat Depression, water depths range between 2 and 3 m, and more than 50 pumping stations are installed on both sides of the canal to facilitate water distribution [5].

Geologically, the development of the Slabiat Depression is believed to be associated with the Abu Jir Fault Zone, where neotectonic movements have played an important role in shaping its present morphology. The northeastern margin of the depression is bordered by the Dibdibba Formation, whereas the southeastern and southwestern margins are bounded by the Nfayil, Ghar, Euphrates, and Dammam formations. Morphometrically, the depression extends for approximately 65 km in length and varies in width from 30 to 32.5 km, reaching its maximum width in the central part. The depth of the depression ranges from 0 to 10 m, reflecting its relatively shallow topography [6].

2. Materials and Methods

2.1 Water Sampling:

Groundwater samples were collected from 19 wells across different areas within the Slabiat Depression. The sampling locations were marked with GPS to ensure precise positioning, and the wells were selected based on their hydrogeological characteristics and proximity to contamination sources Table (1). The collected groundwater samples were analyzed to determine a range of physicochemical parameters, including pH, total dissolved solids (TDS), electrical conductivity (EC), sodium (Na^+), calcium (Ca^{2+}), magnesium (Mg^{2+}), sulfate (SO_4^{2-}), bicarbonate (HCO_3^-), and chloride (Cl^-). Following collection, the samples were transported to the Central Laboratory of the College of Agriculture at Al-Muthanna University and stored in clean two-liter polyethylene bottles prior to analysis. The analytical results were subsequently used to evaluate groundwater quality, identify potential contamination, and determine whether corrective or management measures were required to improve and maintain water quality within the study area.

Table 1. Geographic Coordinates of the Groundwater Sampling Stations in the Slabiat Depression.

No.	station	Easting	Northing
1	S1	45° 14' 51.788"	31° 15' 50.59"
2	S2	45° 17' 54.858"	31° 11' 01.63"
3	S3	45° 12' 41.952"	31° 09' 44.5"
4	S4	45° 27' 18.224"	31° 07' 12.45"
5	S5	45° 33' 57.950"	31° 02' 36.33"
6	S6	45° 34' 11.428"	31° 02' 31.4"

7	S7	45° 37' 07.430''	31° 00' 33.9''
8	S8	45° 39' 18.308''	31° 58' 56.14''
9	S9	45° 39' 06.444''	30° 58' 22.7''
10	S10	45° 39' 40.188''	30° 57' 41.21''
11	S11	45° 40' 44.73''	30° 56' 30.4''
12	S12	45° 44' 44.14''	30° 56' 26.69''
13	S13	45° 47' 43.916''	30° 53' 59.37''
14	S14	45° 49' 16.18''	30° 52' 51.7''
15	S15	45° 48' 22.38''	30° 50' 64.6''
16	S16	45° 50' 16.18''	30° 50' 2.43''
17	S17	45° 46' 22.84''	30° 50' 40.54''
18	S18	45° 43' 23.12''	30° 52' 33.84''
19	S19	45° 42' 12.19''	30° 54' 44.365''

The Water Quality Index (WQI) is used to evaluate water quality. It is a ranking method that provides a composite measure of the overall water quality based on various water quality parameters, expressing water quality both spatially and temporally with a single numerical value. A system based on information entropy theory was applied. Information entropy measures the degree of disturbance in the system, allowing useful data to be evaluated from the presented information . If the difference between objects evaluated on the same parameter is large and the entropy is small, it indicates that more information is available for that parameter, and therefore, it should be assigned a higher weight . The comparative weight would be lower if the entropy were higher and the difference was smaller. Consequently, the weight can be determined objectively using the entropy concept. The primary steps in applying the entropy method to determine weights are as follows:

The following actions are part of the first stage:

1- The normalization process was applied to the original evaluation matrix to standardize the measured groundwater quality parameters and facilitate their comparison. Seven key physicochemical parameters—total dissolved solids (TDS), pH, calcium (Ca^{2+}), magnesium (Mg^{2+}), sodium (Na^{+}), chloride (Cl^{-}), and sulfate (SO_4^{2-})—were selected as indicators of drinking water quality. If (m) water samples are taken to figure out the chemical quality of a certain area. Any sample of water is tested for (n) chemical components (j = 1, 2..., n). The value matrix X can be built from actual data as:

$$\boldsymbol{X} = \begin{vmatrix} x11 & x21 & x1n \\ x21 & x22 & x2n \\ xm1 & xm2 & xmn. \end{vmatrix} \dots\dots\dots\dots\dots. \quad 1$$

To make the data dimensionless and facilitate the comparison of chemical constituents, a standard establishing procedure must be used.

For the cost type (larger values the better)

$$\boldsymbol{yi} = \frac{xi - xi(\min)}{xi(max) - xi(min)} \dots\dots\dots\dots. \quad 2$$

The utilization type, on the other side (smaller values are better)

$$\boldsymbol{yi} = \frac{xi(max) - xi}{xi(max) - xi(min)} \quad \ldots \ldots \ldots \ldots \ldots \quad 3$$

Where: (i) : index (x_i) : Original value of (i)

Xi (max), xi(min) : Maximum and minimum value of original data.

Eq. (2) & (3) normalize the data in the range of 0 and 1. After the process of standardization, the standard-grade matrix (Y) can be made.

$$Y = \begin{matrix} Y\,11 & Y\,21 & Y\,1n \\ y\,21 & y\,22 & y\,2n \\ y\,1 & y\,m2 & y\,mn \end{matrix} \quad \ldots\ldots\ldots \quad 4$$

Here's how to figure out the index value ratio of the (j) index in the (i) sample

$$\boldsymbol{Pij} = \frac{yij}{\sum_{i=1}^{m} yij} \quad \ldots\ldots\ldots\ldots \quad 5$$

2- To explain what entropy is, when ((n)) evaluation indicators and ((m)) evaluation objects are used in a study, the term "entropy of the ((j)) indicator" is used to describe the situation. The information entropy is given in the following way:

$$\boldsymbol{ej} = -\frac{1}{\ln m} \sum_{i=1}^{m} PijLnPij \quad \ldots \ldots \ldots \ldots \quad 6$$

Smallest value of the (ej), is the largest effect of the (j) index, table (2).

3- Definition of the entropy weight. The entropy weight of the ((j) indicator is defined as:

$$\boldsymbol{wij} = \frac{1 - ej}{\sum_{i=1}^{n}(1 - ej)} \quad \ldots \ldots \ldots \ldots \quad 7$$

Table (3) shows the weights for each parameter

The second stage is to determine the quality rating scale (qj) for each parameter of the water quality. The (qj) is calculated a

$$\boldsymbol{qj} = \frac{Cj}{Sj} * 100 \quad \ldots \ldots \ldots \ldots \quad 8$$

where CjC_jCj is the concentration of the jjj-th chemical parameter in each water sample (mg/L), and SjS_jSj is the corresponding WHO drinking water standard shown in Table 3. In the third stage, the Water Quality Index (WQI) is calculated using the weighted linear combination method, which combines the quality ratings and assigned weights of all parameters into a single indicator of overall water quality:

$$\boldsymbol{WQI} = \sum_{j=1}^{n} wij\; qj \quad \ldots \ldots \ldots \ldots \quad 9$$

Table 2. Results of Information Entropy and Parameter Weights.

Parameter	Pij	ej	1−ej	Wij
Na	-1.51891	-0.96147	1.961468	0.111329
K	-1.52842	-0.96748	1.967484	0.111671
Ca	-1.50276	-0.95124	1.951242	0.110749
Mg	-1.47332	-0.93261	1.932611	0.109691
CL	-1.50538	-0.95290	1.952901	0.110843
HCO3	-1.54810	-0.97995	1.979947	0.112378
SO4	-1.51990	-0.96209	1.962094	0.111365

pH	-1.52795	-0.96719	1.967189	0.111654
TDS	-1.49078	-0.94366	1.943663	0.110319

Table 3. Statistical Summary of Hydrochemical Parameters, WHO (2017) Drinking Water Standards, and Relative Weights Assigned to Each Parameter.

Chemical Parameter	Min (Low - high period)	Max (Low - high period)	WHO Standard (Si)	Relative weight (Wi)
Na^+ mg/l	39.1 - 24.6	849.3 - 1748	200	0.03667
K^+ mg/l	17.67 - 5	28.36 - 41.4	20	—
Ca^{2+} mg/l	62.52 - 1748	101 - 361.7	250	0.04956
Mg^{2+} mg/l	24.6 - 119	58.3 - 303.3	50	0.02952
Cl^- mg/l	169.9 - 108.8	369.9 - 305.6	250	0.04295
HCO_3^- mg/l	150 - 151	380 - 289	500	—
SO_4^{2-} mg/l	530 - 411	916 - 699	250	0.06891
pH	8.2 - 7.2	8.7 - 8	6.5 - 8.5	0.15347
T.D.S	1608.32 - 1372	3212.8 - 6520	600	0.53228
EC ds/cm	2513 - 4290	5020 - 10370	500	—

2.2 2D Resistivity Survey

After the fieldwork is over, the field data from the 2-D resistivity imaging study should be processed and interpreted. The PROSYS II software is used to transfer the data file from the resistivity meter's (SYSCAL PRO SWITCH unit) memory to the personal computer. Once field data has been processed, transform the measured and computed apparent resistivity into an inverse model (actual resistivity) that describes the geological subsurface and shows the subsurface resistivity distribution . In order to analyze the field data produced by a 2-D resistivity imaging survey that has numerous factors controlling the demonstration of the final inverse model (actual distribution of subsurface resistivity), numerous contemporary programs have been employed in recent years. PROSYS II and RES2DINV applications are used to process and interpret the field data . Based on numerous wells drilled by the General Commission for Groundwater, prior hydrological studies near the study area, and resistivity table values of common rocks, soil materials, and chemicals, the resistivity values of lithologic formations and groundwater aquifers were estimated.

2-2-1 Removing bad data with RES2DINV program.

1. The file was saved and exported in a format that the RES2DINV application could read after the PROSYS II tool eliminated the abnormally high resistivity values. Before using the inverse subroutine, the RES2DINV program is used in two steps to remove bad data from the data set.
2. Displaying the field data in profile form is the first step in eliminating faulty data, which can be identified as deviating from the field data's overall trend. The file is saved once the faulty data is eliminated by picking it up by the red cross. High-positive bad data values will be higher than the grid's general setting, while negative bad data values will be lower than the grid's general setting.
3. Reducing the RMS error ratio is the second step in eliminating faulty data; the statistic bar chart shows the percentage of apparent resistivity measurement. By moving the green line to the left at the error bar 60%, the 20% or less of poor data in survey can be eliminated. In this manner, the majority of the poor data in survey will be removed before the inverse subroutine iteration is repeated.

3. Results

3.1 Water quality index (WQI)

The different kinds of water quality are identified using the WQI values. The WQI has values between 48 and 581.8. These values were divided into five groups by Sahu and Sikdar (2008), which are shown in table (4).

WQI range	WQI type
< 50	Excellent
50 - 100	Good
100 - 150	Moderate
150 - 200	Poor
> 200	Very poor

Table 5. Water quality index in drinking water of study area.

Dry period			Wet period		
Sample	**Water quality index**	Water-quality	Sample	**Water quality index**	Water - quality
1	163.341	poor	1	179.476	poor
2	162.419	poor	2	189.087	poor
3	181.402	poor	3	166.493	poor
4	190.338	poor	4	266.262	very poor
5	186.871	poor	5	287.749	very poor
6	200.780	poor	6	309.185	very poor
7	187.411	poor	7	311.552	very poor
8	195.834	poor	8	316.713	very poor
9	192.438	poor	9	316.253	very poor
10	189.653	poor	10	325.351	very poor
11	190.973	poor	11	313.061	very poor
12	196.324	poor	12	269.239	very poor
13	176.838	poor	13	326.793	very poor
14	116.258	Moderate	14	371.244	very poor
15	200.249	Very poor	15	327.546	very poor
16	141.969	Moderate	16	330.686	very poor
17	—	—	17	279.199	very poor
18	187.035	poor	18	328.882	very poor
19	—	—	19	290.791	very poor

MIN	116.258	MIN	166.493
MAX	200.780	MAX	371.244
AV	18	AV	289.76

Based on predetermined WQI values, water quality ratings are determined. The average WQI score varies from 180 during the dry time to 289.76 during the wet period. These values are classified as poor to very poor by Jianhua et al. (2011) (Table 4). The results indicated that the Euphrates River and stations 14 and 16 were characterized by moderate to poor water quality during the dry period, whereas the remaining sampling stations generally exhibited better water quality conditions. This variation reflects the spatial differences in hydrochemical characteristics and the influence of seasonal hydrological conditions across the study area., in contrast to the wet season when all samples had water quality ranging from bad to very weak. All stations were deemed to be of low quality during the rainy season. There are numerous factors contributing to the decline in water quality, including factories built on the Euphrates River (the primary feeder), untreated sewage disposal, and numerous other contaminants. The high quantities of dissolved compounds during rainy seasons, when some soil components are dissolved and transferred to river water, are the cause of the decline in water quality. As evidenced by the shift in the element concentration values following station 3, this soil, which is rich in soluble carbonate rocks, greatly contributes to the change in water quality [7].

3.1.2 physical Properties

According to Komatians categorization (2004), the data reveal (Ph) values between (7.1 and 7.6) in Fig. (2), suggesting neutral to mildly alkaline water quality. The pH readings are within the ICOSQC (2009) limiting levels. Furthermore, Fig. (3) shows a significant rise in TDS (Total Dissolved Solids) in the majority of the locations under study, particularly in W1 and W2. Human activity and mixed sewage water are to blame for this growth, which is causing a number of environmental problems. The water is classified as mildly brackish due to the TDS readings, which vary from 5100 to 9010 ppm and exceed the allowable limit of 1000 ppm. Additionally, highly mineralized water due to salinity is indicated by EC (Electrical Conductivity) values between (7123 and 14040) µS/cm (Fig. 4). The permitted ICOSQC limits are exceeded by these EC values. The study's TH (Total Hardness) ranges from 1817 to 3672 ppm (Fig. 5) [8].

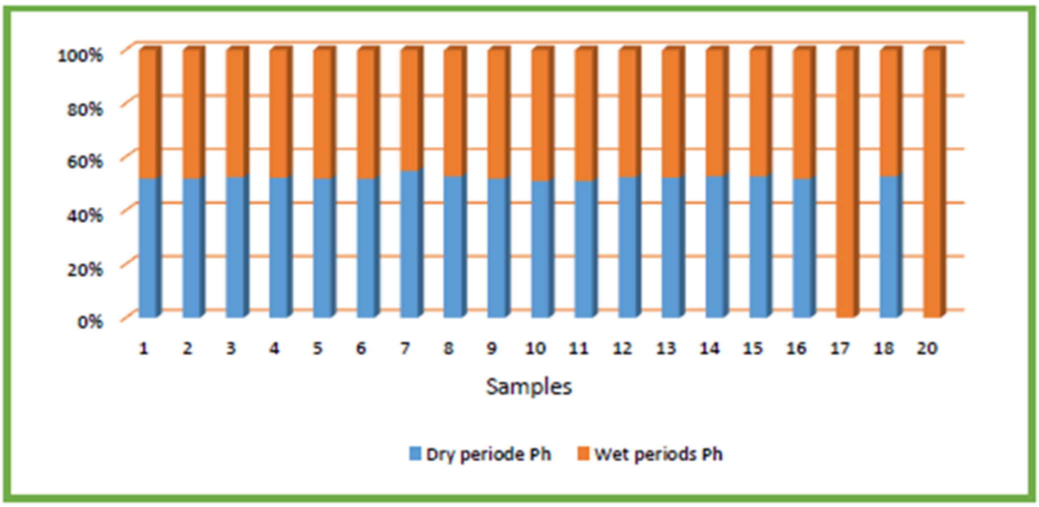

Figure 2. Ph values of the study Area.

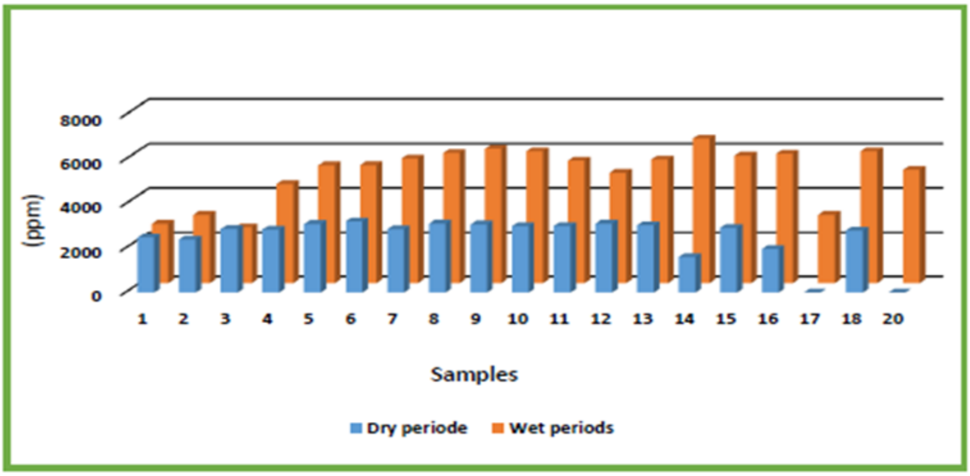

Figure 3. TDS values of the study Area.

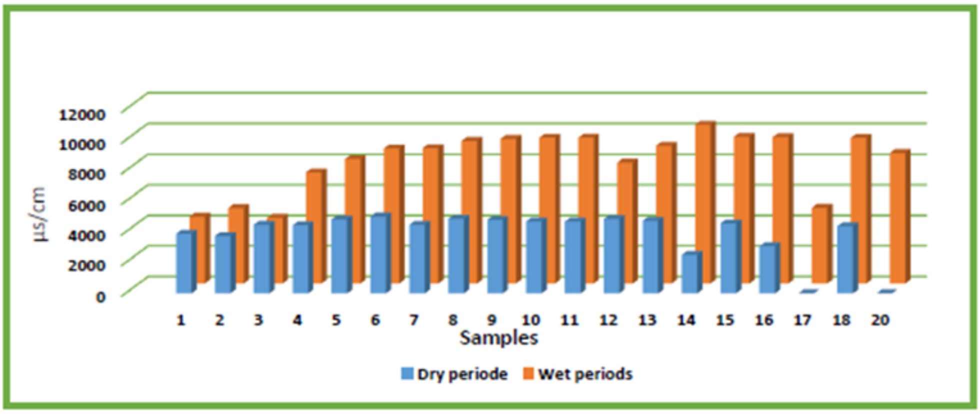

Figure 4. EC values of the study Area.

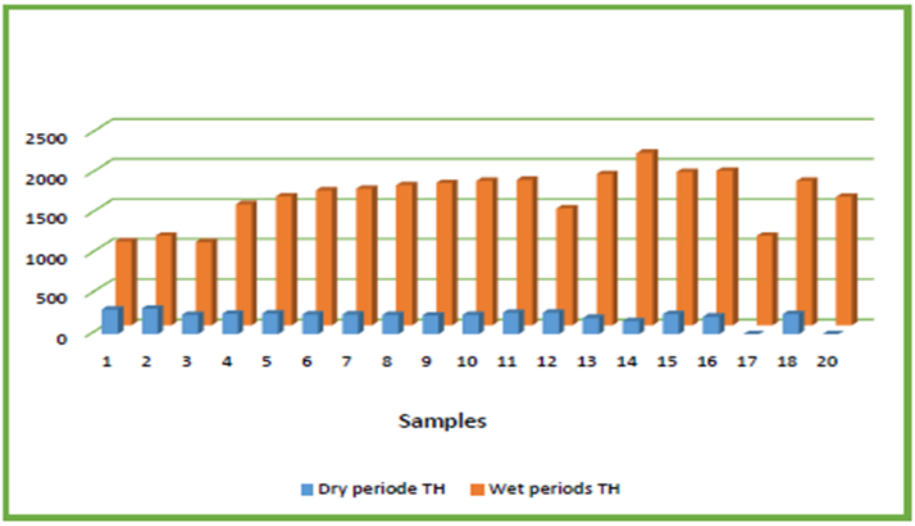

Figure 5. TH values of the study area.

3.1.3 Chemical Properties

The concentrations of Ca2+, Mg2+, and Na2+ in the water samples are displayed in Fig. (6). The research area's calcium concentrations range from 336 to 780 parts per million. The main sources of calcium ions in well water are thought to be human activity and wastewater. Every sample value is higher than the permitted ICOSQC limits. Magnesium ions (Mg^{2+}) are less concentrated than calcium and sodium ions because dolomite dissolves more slowly. magnesium levels ranging from 234 to 420 parts per million. Every sample value exceeds the 50 ppm ICOSQC standard limit (Fig. 7). Sodium is difficult to precipitate and very soluble in water. Wastewater, mineral deposition, and salt intrusion all add sodium to water (WHO, 2017). The range of sodium values in the study region is 678 ppm to 1360 ppm. All of the water samples' salt concentrations are higher than permitted, as seen in Fig [9].

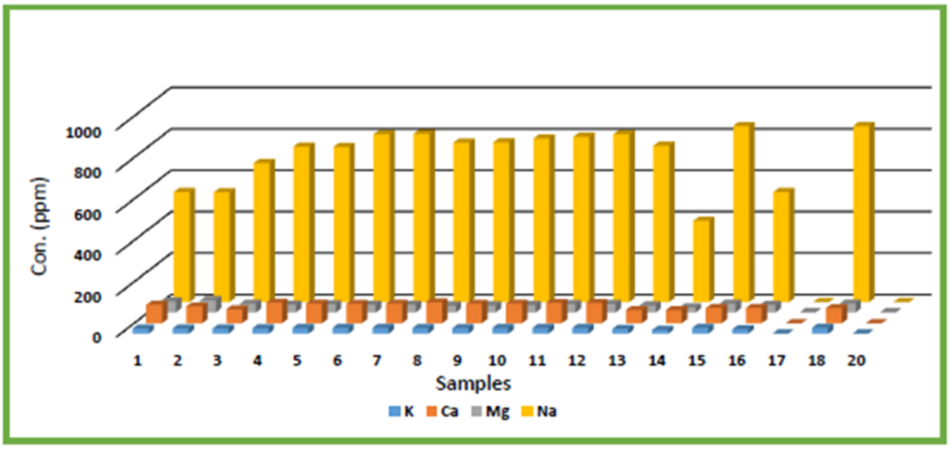

Figure 6. Concentrations of Potassium (K), Calcium (Ca), Magnesium (Mg), and Sodium (Na) at the Sampling Stations in the Study Area During the Dry Period.

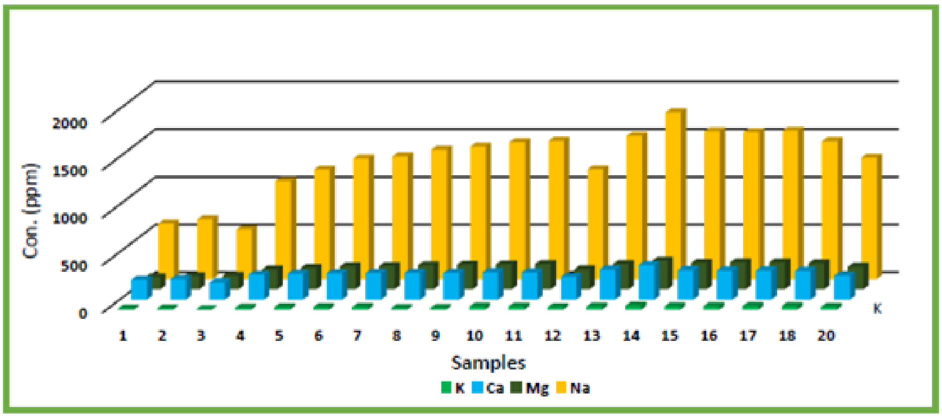

Figure 7. Concentrations of Potassium (K), Calcium (Ca), Magnesium (Mg), and Sodium (Na) at the Sampling Stations in the Study Area During the Wet period.

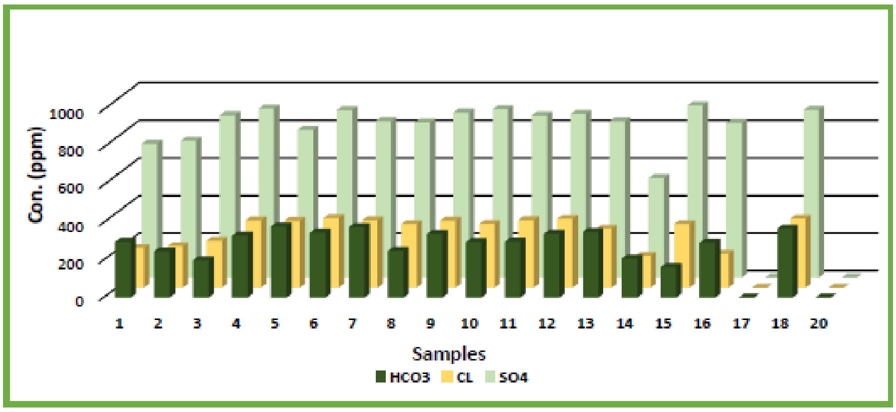

Figure 8. Bicarbonate (HCO_3^-), Chloride (Cl^-), and Sulfate (SO_4^{2-}) Concentrations at the Sampling Stations in the Study Area During the Dry Period.

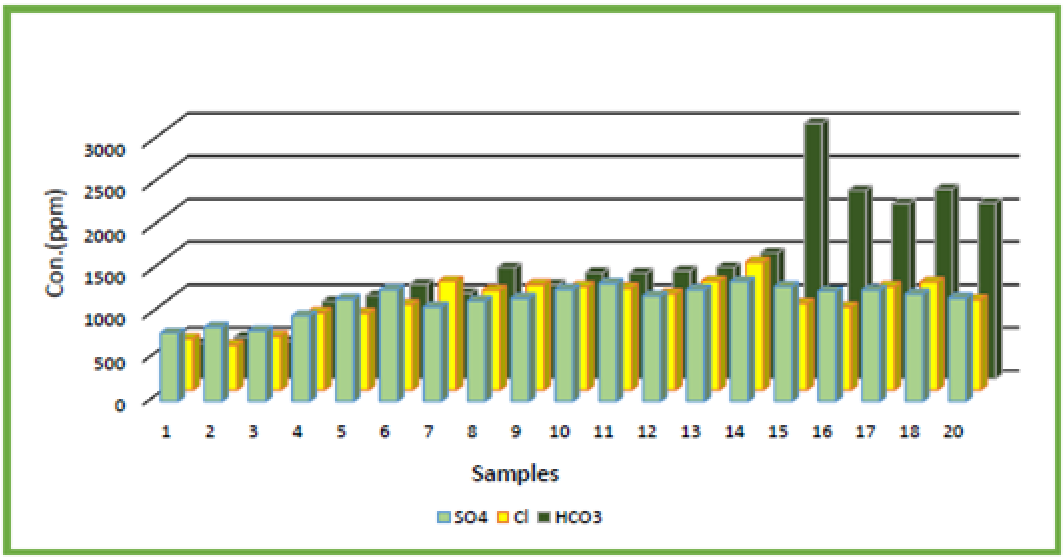

Figure 9. Bicarbonate (HCO_3^-), Chloride (Cl^-), and Sulfate (SO_4^{2-}) Concentrations at the Sampling Stations in the Study Area During the wet period.

3.2 Geophysical

3-2-1 Inversion Parameters.

The RES2DINV program designed to work as much as possible in automatic and powerful manner, due to it has set of default control parameters. It enables the user to adjust field data in order to optimize the inversion subroutine operation. Under the "Change settings" or "Inversion" options, the program's numerous options are grouped into six primary categories. A number of predetermined options, like the damping factors, are included in the application and typically produce good results. However, in certain situations, it achieves superior results by modifying the parameters that govern the inversion subroutine, such as the damping factor's beginning value and minimum value [10]. The study area's noise level and geological makeup determine the damping parameter value. If there is a lot of noise in the survey area, which skews the observed resistivity subsurface values, use a high beginning value of the damping parameter. The final inverse model is obtained by dividing the damping parameter value by the number of iterations. Because the research location is remote from the noise sources, the initial damping filter value utilized with the survey points is (0.2). The damping filter used with the survey points must have a minimum value of 0.02. With each deeper layer, the resolution decreases and the layer thickness increase [11]. In order to prevent the bottom of the deepest layer of the data set from overriding the maximum pseudo-depth, the "Change thickness of layers" option is typically used with the resistivity model. As depth increases, the resolution of the resistivity model decreases, leading to an increased damping factor for deeper layers. The "Optimize damping factor" option minimizes RMS error during iterations. The "Vertical to horizontal flatness filter ratio" is determined by the geological structures' nature. For steeply sloped subsurface structures, the filter value exceeds one, while for horizontal or slightly tilted layers, the value is less than one. In this study area, the geological structures are predominantly horizontal, resulting in a filter value of less than one [12].

4. Discussion

To inverse the field data, there are two primary techniques for optimizing inverse subroutines. The degree of variation in resistivity between adjacent zones, the slope angle of subsurface layers, and the geological context of the survey area all influence the use of any optimization subroutine methods. In subsurface analysis, if layers are horizontal or semi-horizontal with gradual resistance changes, the least-square subroutine is optimal. Alternatively, for layers with steep drops and significant resistance contrasts, such as cavities or metal ores, the Robust subroutine is preferred. This distinction is illustrated in the inverse model of the survey, showcasing clear differences in anomalies between the two methods [13].

The first zone, located at shallow depths, shows low resistivity (2.00 - 4.5 ohm.m), consisting mainly of clay and silt with gypsum, varying in thickness from 10 m in the southwest to 70 m in the northeast. The second zone, believed to be groundwater-bearing, has resistivity between 10.2-51 ohm.m, varying in depth and thickness (50-70 m) within the middle Dammam Formation, extending up to 160 m on one side. The third zone, characterized by high resistivity (over 115 ohm.m), represents the lower Dammam Formation, composed mainly of dolomite and dolomitic limestone Fig. (10).

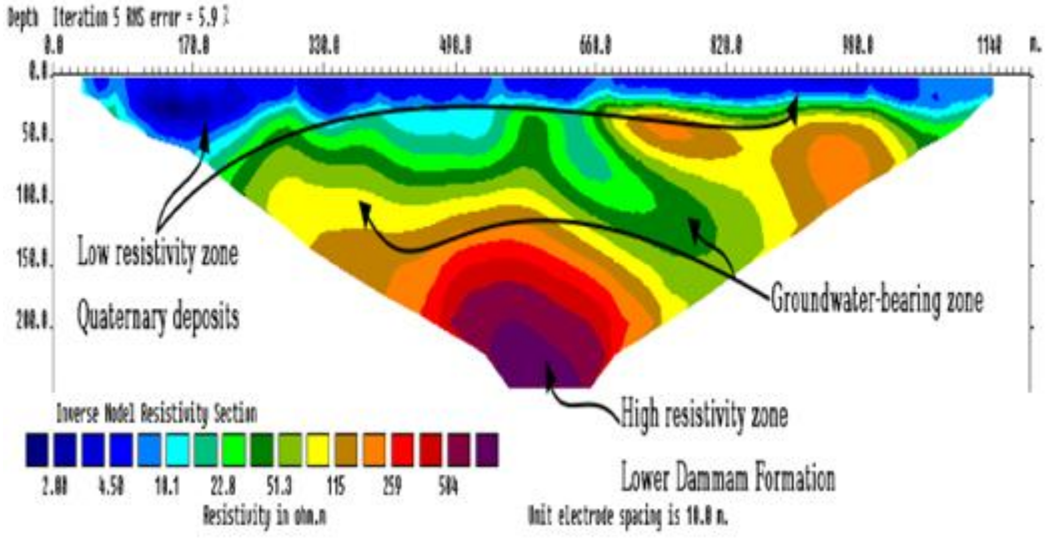

Figure 10. 2D inversion model for first traverse.

The second zone, identified as groundwater-bearing, has resistivity values ranging from (10.2 to 51) ohm.m and varies in depth between 65 and 150 m, situated predominantly beneath a low resistivity zone. It is mainly located on the right side of the inverse model, favored for well drilling. The third zone, characterized by resistivity of (115) ohm.m and higher, is found at the center of the survey point, extending from (100 m to over 200 m) depth, representing the lower Dammam Formation Fig. (11) [14].

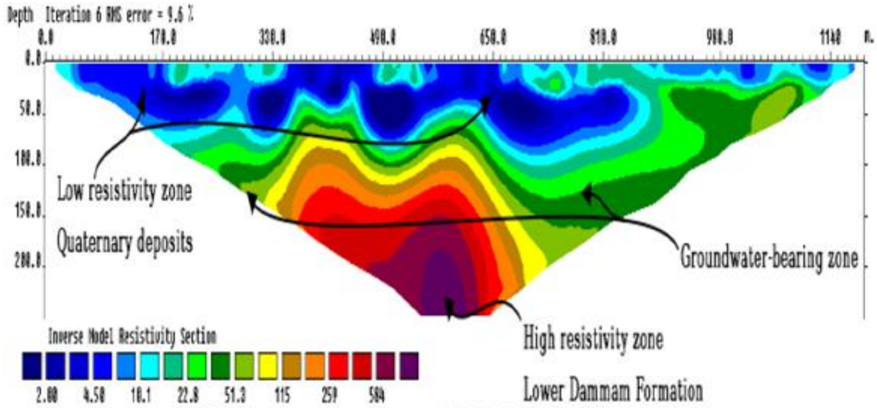

Figure 11. 2D inversion model for second traverse.

The inverse model suggests a fault plane, requiring further geological surveys for confirmation. It divides a high resistivity zone (≥115 ohm.m) on the right into two parts. A groundwater-bearing zone (10.2-51 ohm.m) is found at a depth of (100 m), extending beyond (200 m), mainly within the fault plane. Additionally, a high resistivity zone exists at shallow depths from the surface to 150 m Fig. (12) [15].

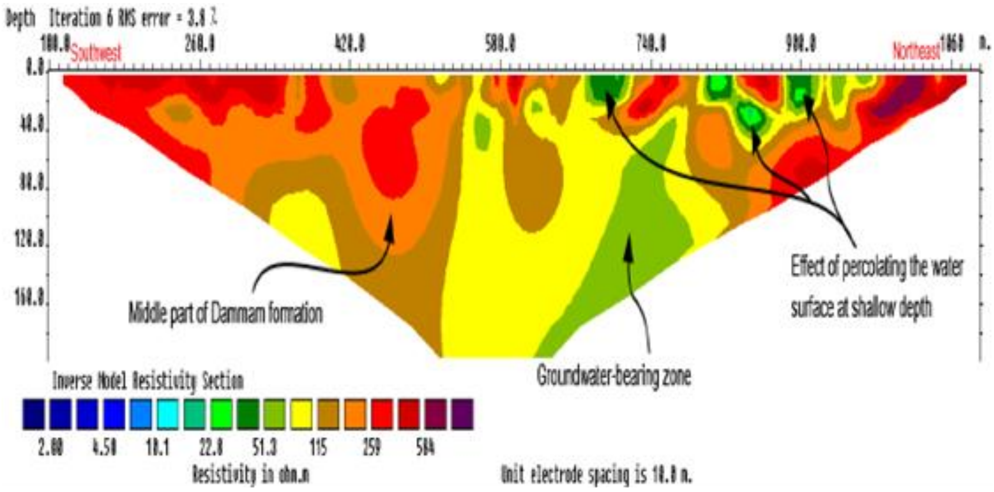

Figure 12. 2D inversion model for third traverse.

5. Conclusion

1. The Euphrates River feeds the Slabiat depression, with concentrations of total dissolved salts rising during wet periods due to soil dissolution processes.
2. Water quality in the area is alkaline, predominantly featuring sulfate and chloride. Although unsuitable for drinking or industrial use, the water can be employed for agricultural irrigation and livestock.
3. The water quality index classifies it as bad to very poor in both dry and wet periods.
4. Because of semi-horizontal subsurface layers and gradual resistivity changes, the optimize Least-squares approach outperforms the optimize Robust method for imaging groundwater-bearing zones.
5. Due to the high conductivity of secondary gypsum and clay minerals, quaternary deposits have low resistivity (2.00-4.5 ohm.m) at varying depths.
6. With the exception of areas where readings are impacted by saline groundwater from the Rus Formation, inverse models show vertical resistivity gradients with higher resistivity at depth.
7. The Dammam formation's middle section has abundant unconfined aquifers due to faults and fractures.
8. The middle Dammam Formation's depth in relation to water levels and fracture degrees is correlated with variations in aquifer thickness and depth among survey stations.
9. A shallow low resistivity zone in the models indicates a decline in quaternary deposit thickness from west to east.
10. Groundwater occurrence is greatly influenced by structural circumstances, which are more common in the west and less common in the east.

REFERENCES

[1] M. M. Ahmed, S. S. Abbas, and A. M. Abed, "Determination of civil engineering problems using resistivity methods in Ramadi, Western Iraq," *Iraqi Geol. J.*, vol. 55, no. 1F, pp. 160–165, Jun. 2022, doi: 10.46717/igj.55.1F.13Ms-2022-06-28.

[2] S. S. Abbas, M. M. Ahmed, A. M. Abed, and F. H. Al-Menshed, "Application of 2D and 3D electrical resistivity imaging techniques for site investigation in Ramadi City, Western Iraq," in *IOP Conf. Ser.: Earth Environ. Sci.*, vol. 1080, no. 1, p. 012011, 2022, doi: 10.1088/1755-1315/1080/1/012011.

[3] S. S. Abbas, H. A. Al-Saady, and W. D. Al-Mahemmdi, "An attempt to delineate subsurface Ain Aldawar cavity using 2D electrical resistivity imaging method in Haditha area, Western Iraq," *Iraqi Geol. J.*, vol. 57, no. 1F, pp. 47–52, Jun. 2024, doi: 10.46717/igj.57.1F.4ms-2024-6-13.

[4] K. G. Andres and R. Canace, "Use of the electrical resistivity technique to delineate a hydrocarbon spill in the coastal plain deposits of New Jersey," in *Proc. NWWA/API Conf. Petroleum Hydrocarbons and Organic Chemicals in Ground Water*, Houston, TX, USA, 1984, pp. 188–197.

[5] M. H. Al-Kubaisi, E. A. Al-Heety, and Y. M. Yousif, "Application of organic indicators and overall index to assess the level of water pollution in Habbaniya Lake, Iraq," *Iraqi Geol. J.*, vol. 54, no. 2A, pp. 93–102, Jul. 2021, doi: 10.46717/igj.54.2A.7Ms-2021-07-28.

[6] M. H. Al-Kubaisi and Q. Y. Al-Kubaisi, "Using SWAT model to estimate the water balance of Wadi Al-Mohammadi Basin, Western Iraq," *Iraqi J. Sci.*, vol. 64, no. 3, pp. 1254–1267, 2023, doi: 10.24996/ijs.2023.64.3.21.

[7] M. Al-Dabbas, Q. Al-Kubaisi, T. Hussein, and S. Al-Qaraghuli, "Hydrochemical properties of ground water of Rahaliya-Ekhedhur region, West Razzaza Lake, Iraq," *MATEC Web Conf.*, vol. 162, p. 05002, 2018, doi: 10.1051/matecconf/201816205002.

[8] M. D. Al-Awsi and Z. T. Abdulrazzaq, "Implementing electrical resistivity tomography to delineate soil contamination zone, Southern Baqubah City, Iraq," *Kuwait J. Sci.*, vol. 49, no. 2, pp. 1–15, Apr. 2022, doi: 10.48129/kjs.10674.

[9] U. Nasir, M. J. Khan, M. Imran, M. R. Khan, and M. Farooq, "Groundwater investigations in the Hattar Industrial Estate and its vicinity, Haripur District, Pakistan: An integrated approach," *Kuwait J. Sci.*, vol. 48, no. 1, pp. 51–61, Jan. 2021, doi: 10.48129/kjs.v48i1.7820.

[10] J. M. Thabit and F. H. Khalid, "Resistivity imaging survey to delineate subsurface seepage of hydrocarbon contaminated water at Karbala Governorate, Iraq," *Environ. Earth Sci.*, vol. 75, no. 1, p. 87, Jan. 2016, doi: 10.1007/s12665-015-4880-y.

[11] T. Dahlin, "The development of DC resistivity imaging techniques," *Comput. Geosci.*, vol. 27, no. 9, pp. 1019–1029, Nov. 2001, doi: 10.1016/S0098-3004(00)00160-6.

[12] Y. Wang, X. Ya, N. Changxin, and D. Lu, "Assessment of chromium waste contamination by electrical resistivity tomography: A case study," *J. Environ. Eng. Geophys.*, vol. 24, no. 1, pp. 163–167, Mar. 2019, doi: 10.2113/JEEG24.1.163.

[13] M. H. Loke, *Tutorial: 2D and 3D Electrical Imaging Surveys*, Geotomo Software, Penang, Malaysia, Tech. Rep., 2016.

[14] R. Z. Jassim and B. S. Al-Jiburi, "Stratigraphy," *Iraqi Bull. Geol. Min.*, vol. 3, special issue, pp. 53–76, 2009.

[15] M. T. Zaini and M. F. Abdul Jab'bar, "Alluvial fans of the Slabiat depression, Iraqi Southern Desert," *Iraqi Bull. Geol. Min.*, vol. 11, no. 1, pp. 79–93, 2015.